Technical Report Documentation Page

1. Report No. ABC-UTC-2016-C3-UNR01 -Final	2. Government Accession No.	3. Recipient's Catalog No.
4. Title and Subtitle **Quantitative Assessment of Soil-Structure Interaction Effects on Seismic Performance of Bridges with ABC Connections**		5. Report Date (e.g., March 2019) January 2023 6. Performing Organization Code
7. Author(s) Emily Lescher, Elnaz Seylabi, Mohamed Moustafa		8. Performing Organization Report No.
9. Performing Organization Name and Address Department of Civil and Environmental Engineering University of Nevada Reno 664 N. Virginia St. Reno, NV 89557		10. Work Unit No. (TRAIS) 11. Contract or Grant No. Enter the correct number: DTRT13-G-UTC41 (for 2013 projects) 69A3551747121 (for 2016 projects)
12. Sponsoring Organization Name and Address Accelerated Bridge Construction University Transportation Center Florida International University 10555 W. Flagler Street, EC 3680 Miami, FL 33174 US Department of Transportation Office of the Assistant Secretary for Research and Technology And Federal Highway Administration 1200 New Jersey Avenue, SE Washington, DC 201590		13. Type of Report and Period Covered Final Report (December 2020 – January 2023) 14. Sponsoring Agency Code
15. Supplementary Notes Visit www.abc-utc.fiu.edu for other ABC reports.		
16. Abstract Successful implementation of accelerated bridge construction techniques in seismic regions can significantly reduce onsite construction time, traffic delays and associated costs. In the past, mostly experimental research has been used to achieve a better understanding of the seismic performance of ABC connections and, recently, full bridge systems. However, none of these studies have taken SSI effects into account causing doubts on the actual performance of these bridges in seismic regions. Moreover, systematic studies that focus on modeling the constitutive behavior of ABC components in numerical simulations are still lacking. To take advantage of rapid bridge construction in seismic areas, such as California, and at the same time improve the resilience of the transportation infrastructure, it is important to consider foundation flexibility as well as well-parametrized constitutive relations in modeling ABC bridge foundations and connections. We consider this proposal as a first step towards developing seismically resilient bridges with ABC connections where we use well-calibrated finite element models to quantitatively assess the effects of SSI on a two-span bridge system with different ABC connection types. The main objective of this project is two-fold: (1) calibration of nonlinear numerical models that could capture the local and global behavior of one of the tested bridge systems, and (2) quantitative assessment of the seismic performance of the selected bridge with taking SSI effects into account		
17. Key Words		18. Distribution Statement

		No restrictions.	
19. Security Classification (of this report) Unclassified.	20. Security Classification (of this page) Unclassified.	21. No. of Pages 36	22. Price

Form DOT F 1700.7 (8-72) Reproduction of completed page authorized

Quantitative Assessment of Soil-Structure Interaction Effects on Seismic Performance of Bridges with ABC Connections

Final Report (January 2023)

Principal Investigator: Elnaz Seylabi and Mohamed Moustafa

Department of Civil and Environmental Engineering, University of Nevada Reno

Authors

Emily Lescher, Elnaz Seylabi, Mohamed Moustafa

Sponsored by

Accelerated Bridge Construction University Transportation Center

A report from

University of Nevada Reno
Department of Civil and Environmental Engineering, MS 258
1664 N. Virginia St.
Reno, NV 89557

Disclaimer

The contents of this report reflect the views of the authors, who are responsible for the facts and the accuracy of the information presented herein. This document is disseminated in the interest of information exchange. The report is funded, partially or entirely, by a grant from the U.S. Department of Transportation's University Transportation Program. However, the U.S. Government assumes no liability for the contents or use thereof.

Abstract

Accelerated bridge construction (ABC) utilizes prefabricated members to reduce construction time and overall project expenses. The connection between the prefabricated members has been studied for multiple ABC connections, but no studies have investigated a bridge system with ABC connections on the soil. This project conducts a quantitative assessment of soil-structure interaction (SSI) effects on the seismic performance of bridges with ABC connections. To achieve this objective, the outcome of a recently completed ABC-UTC project is used to develop a baseline finite element model for a two-span bridge system with six ABC connection types. The experimental data are used to validate the baseline finite element model. To model foundation flexibility, the direct modeling approach is used to model the surrounding soil and incident wavefield.

Consequently, a series of numerical experiments are performed to assess the seismic performance of ABC connections and the bridge system, considering SSI effects. The results suggest that for the cases studied in this project, SSI may reduce the demands for the connections significantly in the longitudinal direction and slightly in the transverse direction. Further studies are needed to take more complex site conditions into account.

Acknowledgments

This project was supported by the Accelerated Bridge Construction University Transportation Center (ABC-UTC) at Florida International University as the lead institution. The authors would like to acknowledge the ABC-UTC support. The authors would also like to thank Dr. Saiid Saiidi and Dr. Elmira Shoushtari for providing the experimental and analytical data for the previously completed ABC-UTC project on shake table studies of a bridge system with ABC connections.

Table of Contents

Introduction

Researchers have studied ABC connections using analytical and experimental studies. Most of these studies have focused on the connections' local response without looking at how the connections work in a bridge system. To better understand the response of the ABC connections and incorporate the connections into bridge construction, the connections must be analyzed under realistic seismic loading contrary to uni-directional loading. On the other hand, there is limited knowledge about the performance of bridges with ABC connections in response to soil-structure interaction (SSI) effects. This research aims to shed light on the seismic response of bridges with ABC connections with and without SSI effects.

Shoushtari et al. (2019) performed large-scale shake table experiments to study the performance of six ABC connections in a bridge system under realistic earthquake excitation (no SSI effects included). The bridge model was a 0.35 scale model of a typical two-span prototype bridge. The model was constructed and tested on shake tables at the University of Nevada, Reno. Figure 1 shows a three-dimensional view of the model bridge used for testing.

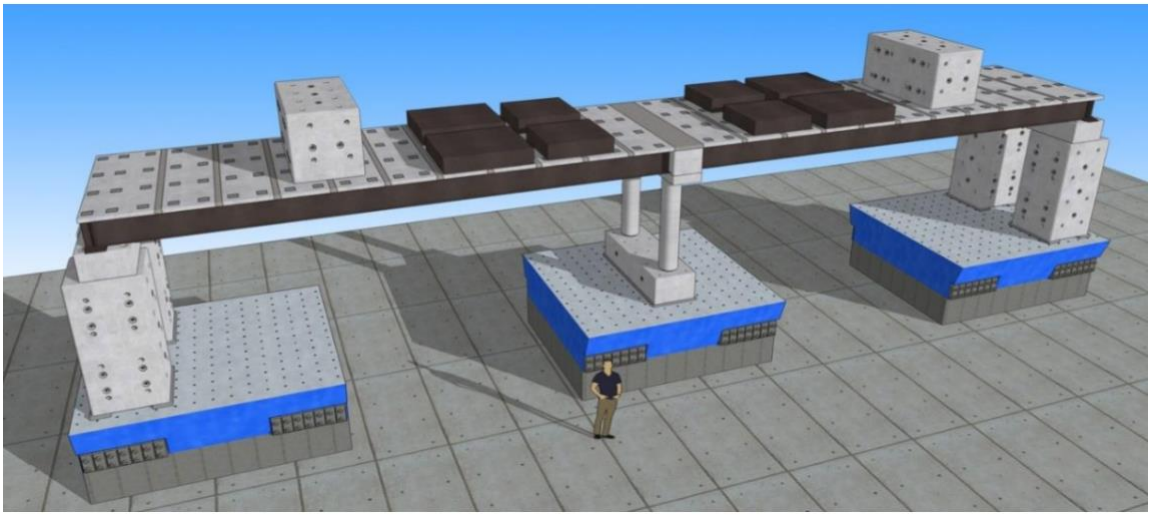

Figure 1: Three-dimensional test setup by Shoushtari et al. (2019)

The bridge model consists of two equal spans of 34.67 ft (416 in.) and is 11 ft (132 in.) wide. The bridge is supported by a two-column bent in the center and seat-type abutments at each end. The bent consists of two 1.33 ft (16 in.) diameter columns with a clear height of 7ft (84 in.) spaced 6.5 ft (78 in.) apart on-center and a 2 ft (24 in.) wide by 2.5 ft (30 in.) deep cap beam that spans the entire width of the bridge. The columns are designed to have pin connections at the base and are integral with the superstructure. The superstructure comprises four steel plate girders with a 2.75-in. deck overlay of 22 precast deck panels.

Lead pallets and concrete blocks were placed on the deck as superimposed mass to replicate the weight of the prototype bridge. The mass consisted of 63 kips of lead pallets and 37 kips of concrete blocks. The mass of the lead was distributed between eight pallets, and the mass of the concrete was distributed between two blocks. The masses were strategically placed to replicate the dead loads of the prototype bridge. Twenty-two string potentiometers and six tri-axial accelerometers were placed at the bridge's abutments, pier, and midspans to record the structure's displacements and accelerations. Figure 2 shows the layout of where the string potentiometers and accelerometers are placed along the bridge. The data recorded from testing was used to evaluate the overall bridge response.

The model bridge consists of six different ABC connections: rebar hinge pocket connection, grouted duct connection, simple for dead continuous for live (SDCL) girder-to-cap beam connection, girder-to-deck grouted pocket connection, ultra-high-performance concrete (UHPC)-filled joints between the deck panels, and deck panel UHPC-filled connection above the pier. Figure 3 shows a schematic of the bridge with all ABC connections used in testing. The ABC

connection design details can be found in Shoushtari et al. (2019). We will use the results of this experimental work to develop the scaled and prototype bridge models to study the SSI effects.

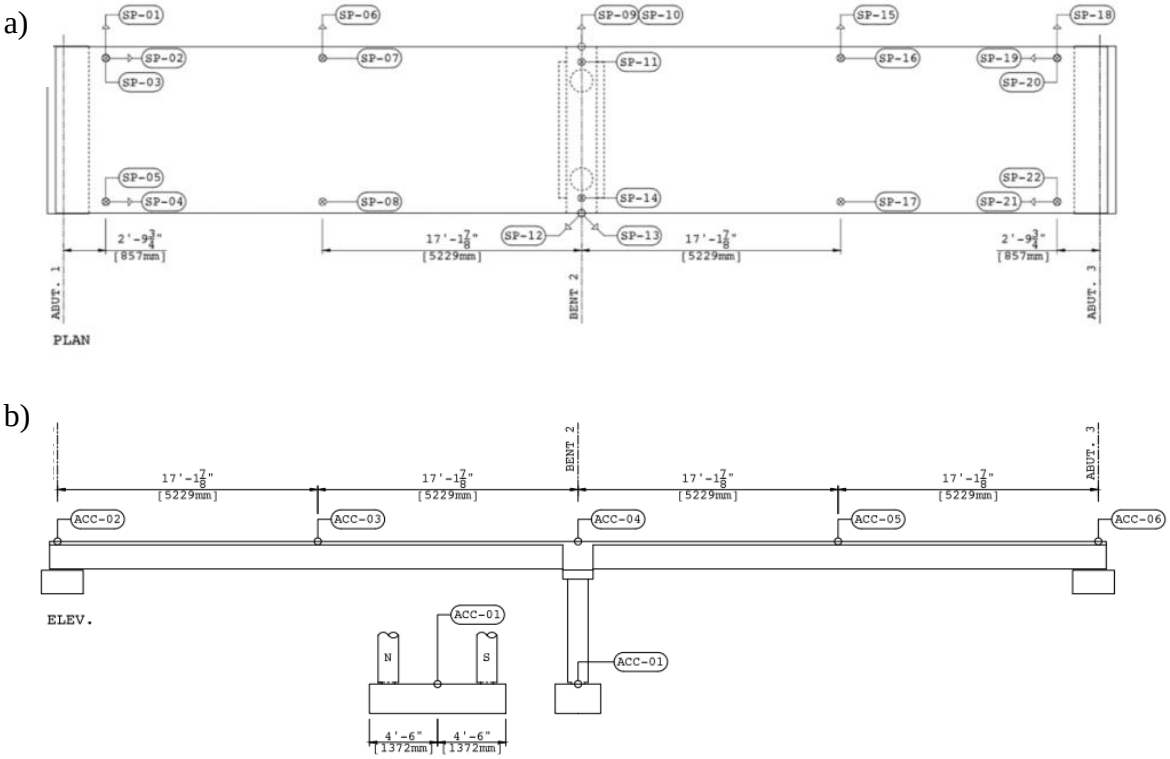

Figure 2: Layout of a) string potentiometers and b) accelerometers (from Shoushtari et al., 2019).

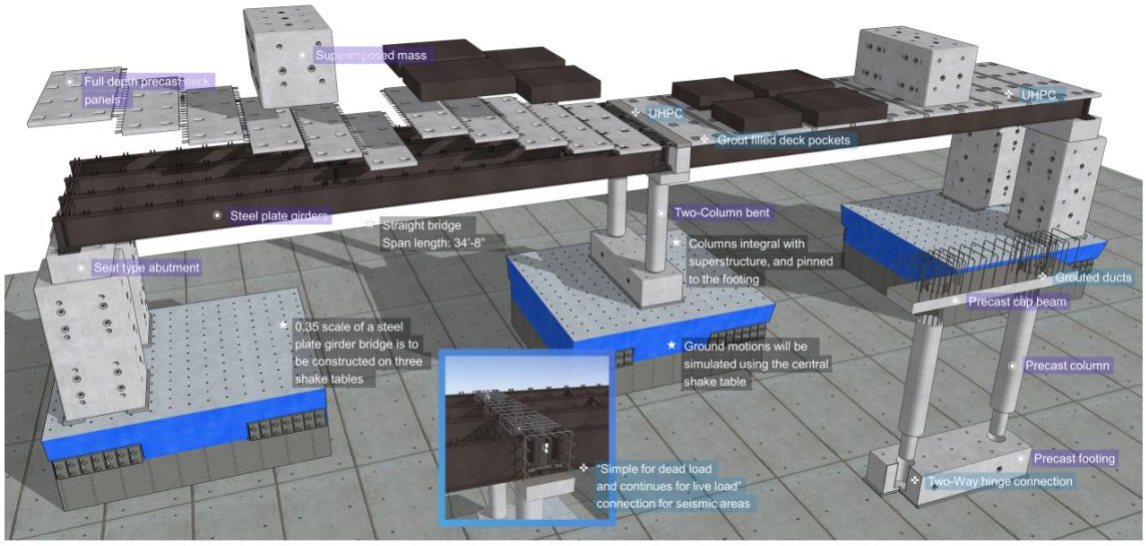

Figure 3: Layout of ABC connections used in testing (Shoushtari et al., 2019).

Two commonly used methods for analyzing the response of bridges on soil are direct, and substructure modeling approaches. The direct modeling method explicitly models the structure, foundations, and surrounding soil, while the substructure modeling approach replaces the surrounding soil with a series of springs and dashpots. Both approaches have been used to study SSI effects on bridges. For instance, for modeling the response of the Meloland bridge system, Kwon and Elnashai (2008) used a multiplatform approach for direct modeling of a bridge-soil system, where they used the OpenSees software to model the soil domain, pile groups, and pile caps and Zeus-NL software was used to model the structural components of the bridge (Figure 4). Rahmani et al. (2014), on the other hand, used a single platform, i.e., OpenSeesSP, for the direct modeling of the same bridge (Figure 5). The results from the 3D continuum model were like the multiplatform study by Kwon and Elnashai (2008). Using the substructure method, Mylonakis et al. (1997) analyzed two different bridge-pier systems, including a single drilled pile and a pile group with a pile cap – their results show that ignoring the radiation damping due to inclusion of SSI effects may lead to overprediction of acceleration response at the deck and pile bending moment up to 50%. Among these two approaches, the direct modeling approach is more rigorous and will be used for modeling the SSI effects in this study.

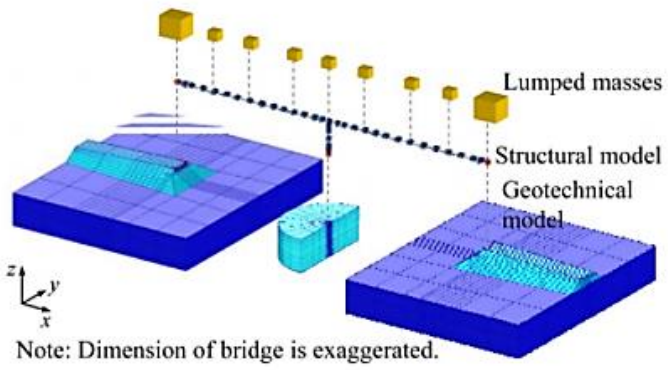

Figure 4: Configuration of the finite element models for the multiplatform analysis (Kwon and Elnashai, 2008).

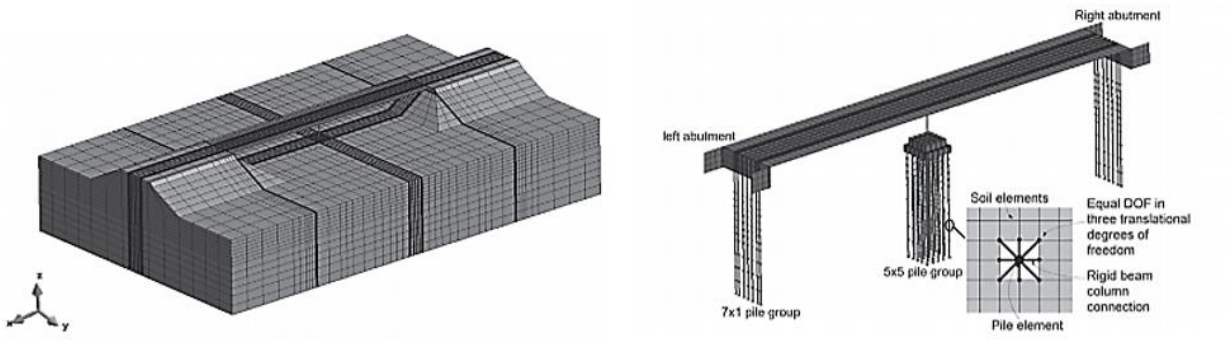

Figure 5: Finite element model of the bridge and soil domain (Rahmani et al., 2014).

With this introduction, in the following sections, details of the scaled bridge model developed in OpenSees are provided, based on the two-span 0.35-scale bridge with six ABC connections tested by Shoushtari et al. (2019). The experimental data of that study is used to validate the developed model's capability in capturing main response quantities. Then, the validated model is scaled up to develop a finite element model of a prototype scale two-span bridge to study the SSI effects on the bridge response, especially at the base connections.

Scaled Bridge Model

The Open System for Earthquake Engineering Simulation (OpenSees) finite element package was used to develop a simplified wireframe model of the bridge (McKenna et al., 2010). The three-dimensional view of the simplified model is shown in Figure 6. Frame elements were used to model the deck, cap beam, and columns. The materials for the elements were defined using the predefined "Concrete02" and "Steel02" materials for the concrete and steel reinforcement, respectively. The concrete has a specified compressive strength of 9.3 ksi, and the steel was specified as Grade 60 with a yield stress of 68 ksi to match the material properties used in the Shoushtari et al. (2019).

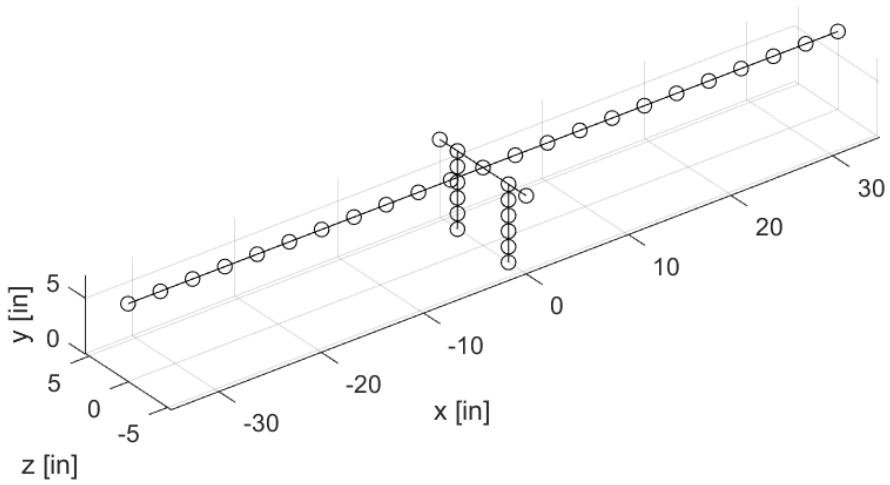

Figure 6: Three-dimensional view of the simplified wireframe bridge model

The column section is a fiber section using a circular patch for the concrete and a circular layer for the longitudinal reinforcement. The concrete is defined for the entire 16 in. diameter, and the reinforcement is defined as 12 No. 5 bars with an inch cover. The torsion for the section is defined by the concrete shear modulus and polar moment of inertia. Five displacement-based beam-column elements are used to define each column. The bottom nodes are free to rotate, and the top nodes are integral with the cap beam.

The cap beam section is defined as a fiber section using a quadrilateral patch for the concrete and straight layers for the reinforcement. The beam has a cross-section of 2.5 ft in height by 2 ft in width. The concrete is defined for the entire section, and the reinforcement is defined with two layers of 6 No. 5 bars, one at the top and one at the bottom. The torsion for the section is defined by the concrete shear modulus and polar moment of inertia. The cap beam consists of four force-based beam-column elements.

The deck and girders were simplified to a single line of elements. Two elements are defined at each location: one for the deck overlay and one for the girders. The deck properties were modeled

in SAP2000 and used to create elastic sections. The plan and elevation views of the SAP2000 model are shown in Figure 7. The deck was modeled as a 2.75 in. thick by 11 ft wide slab shell section with a single layer of No. 3 rebar. The shell section spans the entire length of the bridge. The section properties for the deck are shown in Figure 8.

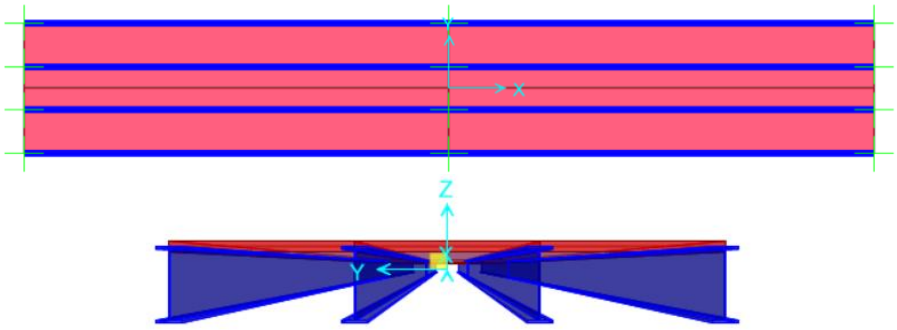

Figure 7: Plan and elevation views of the superstructure in SAP2000

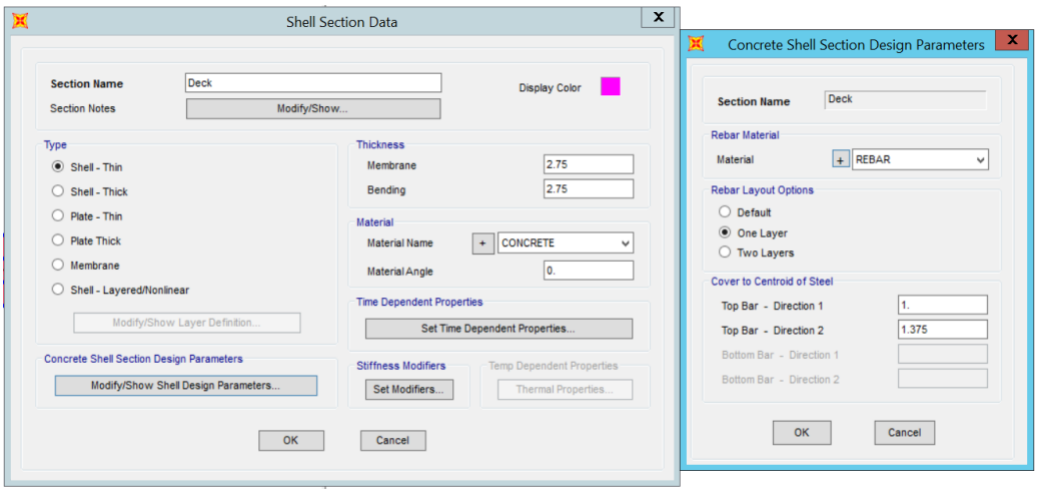

Figure 8: Deck overlay properties

The four steel girders are defined as wide flange frame sections with a steel yield stress of 50 ksi and elastic modulus of 29000 ksi. The girders are spaced evenly across the width of the bridge. Each girder has a total height of 19.25 in. with 0.625 in. thick by 6 in. wide flanges. The dimensions are the same as the tested model bridge and are shown in Figure 9. The deck and girders are defined

as two separate elastic sections in OpenSees. The cross-sectional area, the moment of inertia about the y-axis, and the moment of inertia about the z-axis were determined from the SAP2000 output for the four girders and deck. Since the girder element is a single line, the moment of inertia about the y-axis and z-axis were recalculated using the parallel axis theorem. Table 1 shows the property values used for the deck and girder sections. The superstructure is defined as two separate force-based beam-column elements between 22 nodes. The end nodes are restrained vertically to act as seat-type abutments.

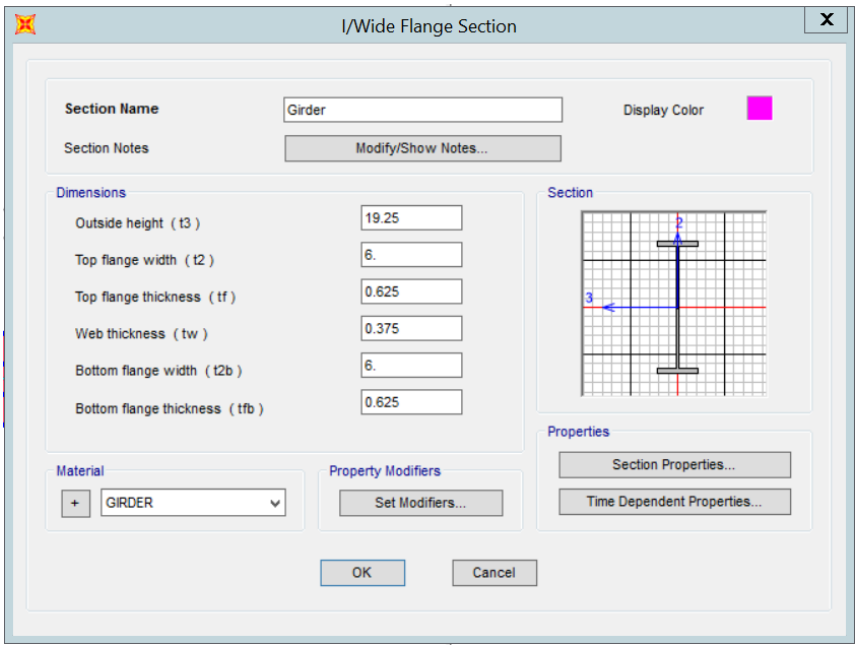

Figure 9: Girder dimensions

Table 1: Section properties for the deck and girders

Property	Deck	Girders
Area (in^2)	363.0	57.0
Iy (in^4)	1022.3	8524.7
Iz (in^4)	527076.0	138030.4
J (in^4)	528098.3	146555.1

For the analysis, the mass of the bridge deck is lumped at the nodes, and the mass of the column is distributed through the displacement-based beam-column elements. The superimposed mass from the concrete blocks and lead pallets is distributed to the corresponding nodes. The computed weight of each column and the cap beam is 1.46 kips and 7.3 kips, respectively. The total weight of the deck and girders computed by SAP2000 is 38.75 kips. For the gravity analysis, the load at each node is applied only in the vertical direction (y-direction). The loads are divided by gravity to calculate the mass at the corresponding nodes. The mass is applied to the x-, y-, and z-coordinates.

The OpenSees wireframe model was tested to estimate the nonlinear response of the bridge and to compare the results to the recorded data as validation. The model was subjected to the ground motion recording applied to the experimental bridge. The input ground motion applied in the longitudinal and transverse directions is shown in Figure 10. The input ground motion is from the 1994 Northridge, California earthquake. The experimental bridge was subjected to eight different runs with peak ground accelerations (PGA) ranging from 0.10 g to 0.82 g and 0.08 g to 0.80 g in the longitudinal and transverse directions, respectively. Run 4 and 8 simulate 125% and 225% of the design-level earthquake. Although the wireframe model was subjected to all eight runs, the results from run 4 and run 8 are used to analyze how well the model captures the nonlinear response.

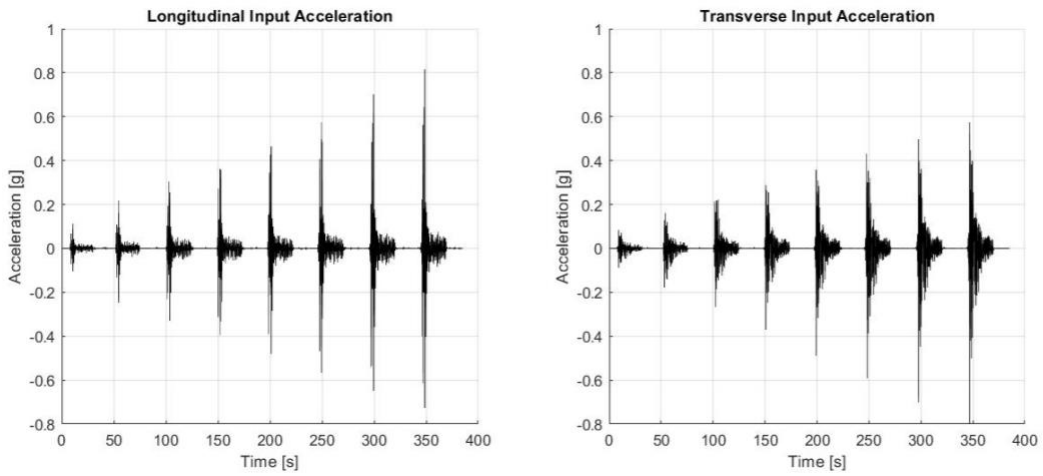

Figure 10: Input acceleration in the longitudinal and transverse directions for the OpenSees model.

The response of the stick model bridge is determined by placing recorders where the string potentiometers are located on the experimental bridge. The recorders record the relative displacement in both the longitudinal and transverse directions. The results from the recorders are used to create an animation of the bridge response to ensure the bridge motion is accurate. The wireframe model was modeled in two ways: with a single line of elements for the superstructure and a single line of two elements for the superstructure.

Both models were tested with 4% and 6% damping to determine which model captured the response with the most accuracy. Figure 11 shows the locations of the displacement recorders on the model in the plan view. Rayleigh damping is used to define the damping of the model. The damping is determined using the natural frequencies from the first and fifth modes. Table 2 and Table 3 show the maximum results of the displacement recorders for four different simplified models for 4% damping and 6% damping: A) shake table testing, B) pinned columns with a single element deck, C) fixed columns with single element deck, D) pinned columns with two element deck, and E) fixed columns with two element deck. The results show that the stick model with pinned columns and two elements along the bridge deck (Model D) has the best accuracy for

capturing the maximum displacement response. Model D was chosen for further comparison with the test results.

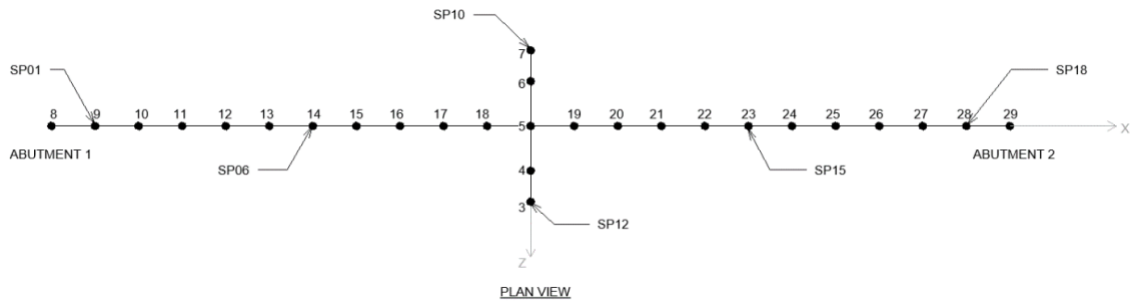

Figure 11: Location of transverse displacement recorders used for response comparisons.

Table 2: Maximum displacement comparison for 4% damping

			Results for 4% damping					Percentage of error compared to test results					
	Model	Identifier	SP01	SP06	SP10	SP12	SP18	SP01	SP06	SP10	SP12	SP18	Transverse Average
RUN 4	**Test Results**	**A**	2.152	1.995	1.865	2.698	1.878	-	-	-	-	-	-
	Simple 1 - Pinned	B	2.764	2.662	2.564	2.559	2.444	24.9%	28.6%	31.6%	5.3%	26.2%	**23.3%**
	Simple 1 - Fixed	C	0.561	0.543	0.539	0.532	0.678	117.3%	114.4%	110.3%	134.1%	93.9%	**114.0%**
	Simple 2 - Pinned	D	2.731	2.648	2.567	2.562	2.462	23.7%	28.1%	31.7%	5.2%	26.9%	**23.1%**
	Simple 2 - Fixed	E	1.110	1.023	0.937	0.940	0.961	64%	64%	66%	97%	65%	**71%**
RUN 8	**Test Results**	**A**	4.237	4.110	3.906	4.055	3.705	-	-	-	-	-	-
	Simple 1 - Pinned	B	4.470	4.406	4.347	4.342	4.312	5.4%	7.0%	10.7%	6.8%	15.1%	**9.0%**
	Simple 1 - Fixed	C	3.496	3.427	3.429	3.427	3.583	19.2%	18.1%	13.0%	155.3%	3.3%	**41.8%**
	Simple 2 - Pinned	D	4.374	4.335	4.297	4.292	4.281	3.2%	5.3%	9.5%	5.7%	14.4%	**7.6%**
	Simple 2 - Fixed	E	3.455	3.455	3.458	3.457	3.580	20.3%	17.3%	12.2%	15.9%	3.4%	**13.8%**

Table 3: Maximum displacement comparison for 6% damping

			Results for 6% damping					Percentage of error compared to test results					
	Model	Identifier	SP01	SP06	SP10	SP12	SP18	SP01	SP06	SP10	SP12	SP18	Transverse Average
RUN 4	**Test**	**A**	2.152	1.995	1.865	2.698	1.878	-	-	-	-	-	-
	Simple 1 - Pinned	B	2.673	2.581	2.494	2.488	2.394	21.6%	25.6%	28.8%	8.1%	24.2%	**21.7%**
	Simple 1 - Fixed	C	0.572	0.538	0.518	0.510	0.624	116.0%	115.1%	113.1%	136.5%	100.3%	**116.2%**
	Simple 2 - Pinned	D	2.660	2.585	2.512	2.507	2.423	21.1%	25.8%	29.6%	7.3%	25.4%	**21.8%**
	Simple 2 - Fixed	E	0.707	0.630	0.559	0.559	0.706	101%	104%	108%	131%	91%	**107%**
RUN 8	**Test**	**A**	4.237	4.110	3.906	4.055	3.705	-	-	-	-	-	-
	Simple 1 - Pinned	B	4.398	4.338	4.282	4.277	4.253	3.7%	5.4%	9.2%	5.3%	13.8%	**7.5%**
	Simple 1 - Fixed	C	3.350	3.215	3.216	3.214	3.368	23.4%	24.4%	19.4%	23.1%	9.5%	**20.0%**
	Simple 2 - Pinned	D	4.315	4.278	4.241	4.236	4.229	1.8%	4.0%	8.2%	4.4%	13.2%	**6.3%**
	Simple 2 - Fixed	E	3.279	3.276	3.278	3.277	3.396	25%	23%	17%	21%	9%	**19%**

Model D results compare the modal analysis, maximum displacements, and hysteresis curves in the longitudinal and transverse directions to the experimental results. The first three modes are in-plane rotation, longitudinal, and transverse, with periods agreeing with the modal analysis results

provided by Shoushtari et al. (2019) (Table 4). The first three mode shapes for the simplified model are shown in Figure 12.

Table 4: Corresponding periods for the first three modes.

Mode	This Study	Shoushtari et al. (2019)
1	1.42 s	1.38 s
2	0.38 s	0.37 s
3	0.27 s	0.27 s

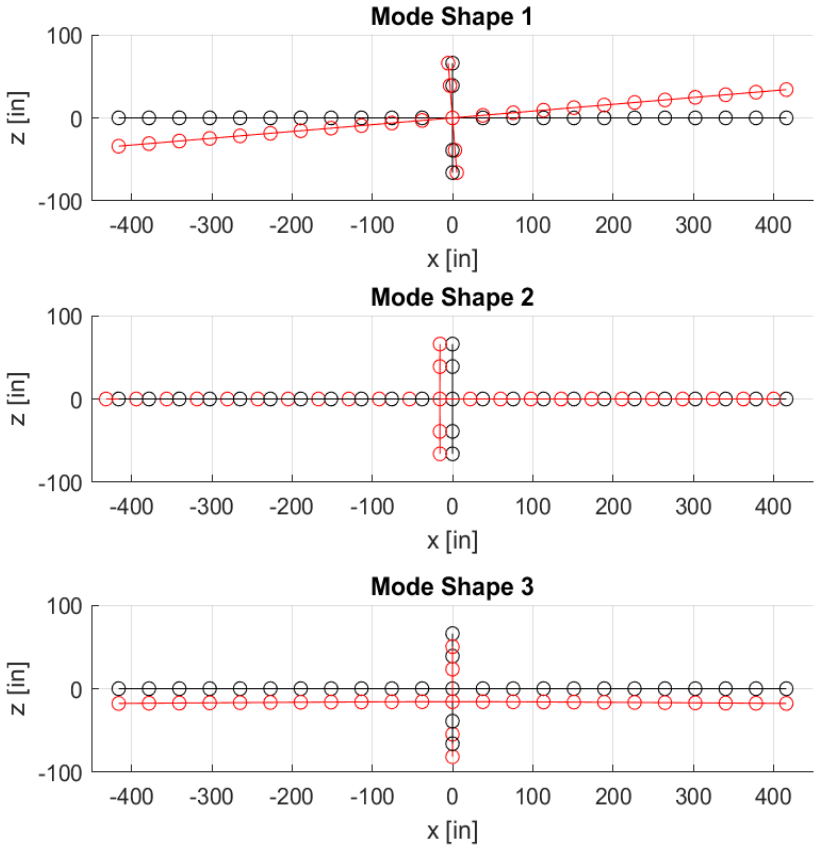

Figure 12: First three mode shapes of the wireframe model

Model D was also subjected to the input ground motions with 4%, 6%, and 8% damping for run 4 and run 8. The damping was increased to 8% to determine if higher damping resulted in better estimates of relative displacements. Table 5 compares the maximum relative displacements of the

wireframe model in the transverse direction to the experimental data. The results show that 8% damping can capture the maximum transverse displacements within a 10 percent error.

Table 5: Transverse displacement results of Model D compared to the experimental data.

	Maximum displacement comparison for two element deck							Percentage of error compared to test results						
	Model	SP01	SP06	SP10	SP12	SP15	SP18	SP01	SP06	SP10	SP12/13	SP15	SP18	Transverse Average
RUN 4	**Test Results**	**2.152**	**1.995**	**1.865**	**2.698**	**1.855**	**1.878**	-	-	-	-	-	-	**-**
	Simple - 4% Damping	2.731	2.648	2.567	2.562	2.514	2.462	23.7%	28.1%	31.7%	5.2%	30.2%	26.9%	**23.1%**
	Simple - 6% Damping	2.660	2.585	2.512	2.507	2.467	2.423	21.1%	25.8%	29.6%	7.3%	28.3%	25.4%	**21.8%**
	Simple - 8% Damping	2.046	1.983	1.923	1.918	1.887	1.855	5.1%	0.6%	3.1%	33.8%	1.8%	1.2%	**8.8%**
RUN 8	**Test Results**	**4.237**	**4.110**	**3.906**	**4.055**	**3.827**	**3.705**	-	-	-	-	-	-	**-**
	Simple - 4% Damping	4.374	4.335	4.297	4.292	4.289	4.281	3.2%	5.3%	9.5%	5.7%	11.4%	14.4%	**7.6%**
	Simple - 6% Damping	4.315	4.278	4.241	4.236	4.235	4.229	1.8%	4.0%	8.2%	4.4%	10.1%	13.2%	**6.3%**
	Simple - 8% Damping	3.801	3.754	3.711	3.702	3.695	3.684	10.8%	9.1%	5.1%	9.1%	3.5%	0.6%	**6.9%**

The hysteresis loops use the reactions generated at the bottom of the columns and the relative displacements at the top of the columns to generate a force versus displacement plot. Recorders are used in OpenSees to calculate the reactions and displacements, which are then averaged to determine the response for the center of the bent. Figure 13 shows the hysteresis loop from run 1 to run 8 with the associated backbone curves overlaid for the longitudinal and transverse directions. Figure 14 shows the associated backbone curves for the wireframe model compared to the recorded test data. The longitudinal curve strongly agrees with the wireframe model and test data. The transverse backbone curve shows that the wireframe model, within reasonable error, captures the peak values. These results validate that the developed wireframe model can be used to capture the response of a texted bridge subjected to earthquake time histories. In the next section, the model's design is rescaled to a prototype bridge to study SSI effects.

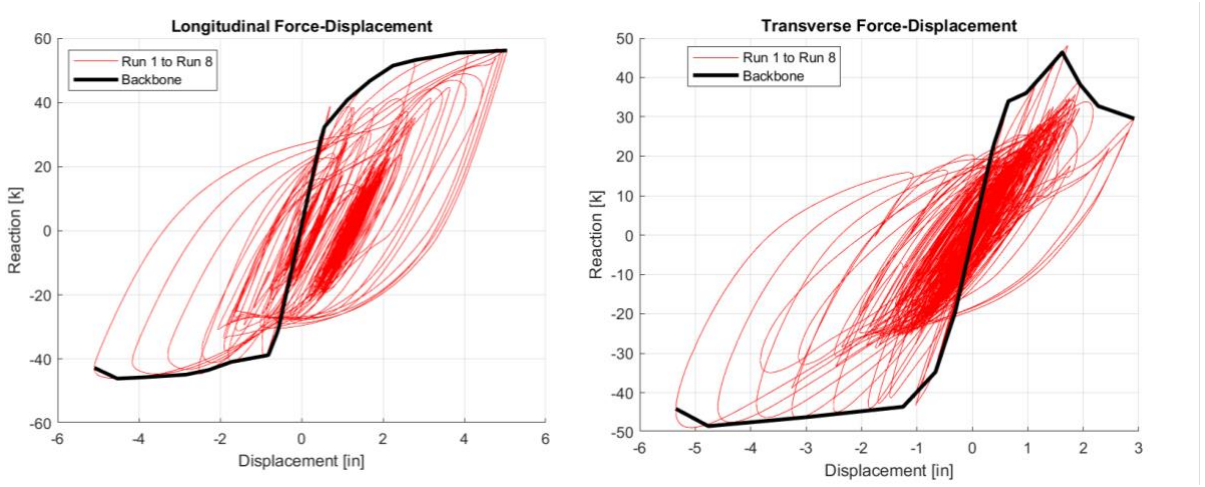

Figure 13: Longitudinal and transverse hysteresis loops for the analytical wireframe model with associated backbones.

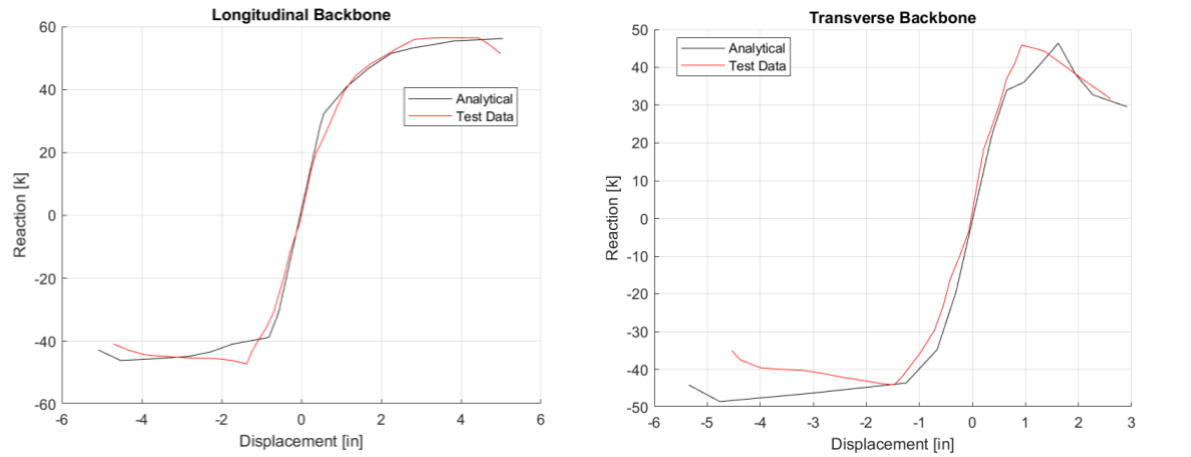

Figure 14: Associated backbone curves for the analytical wireframe model and test data in the longitudinal and transverse directions.

Prototype Bridge Model with Fixed Base

The simplified wire bridge model is scaled up to the prototype scale to analyze the response with and without a soil domain present. Figure 15 shows the elevation view of the prototype bridge that Shoushtari et al. (2019) used for scaling purposes. The prototype bridge consists of the same four girders with deck overlay superstructure.

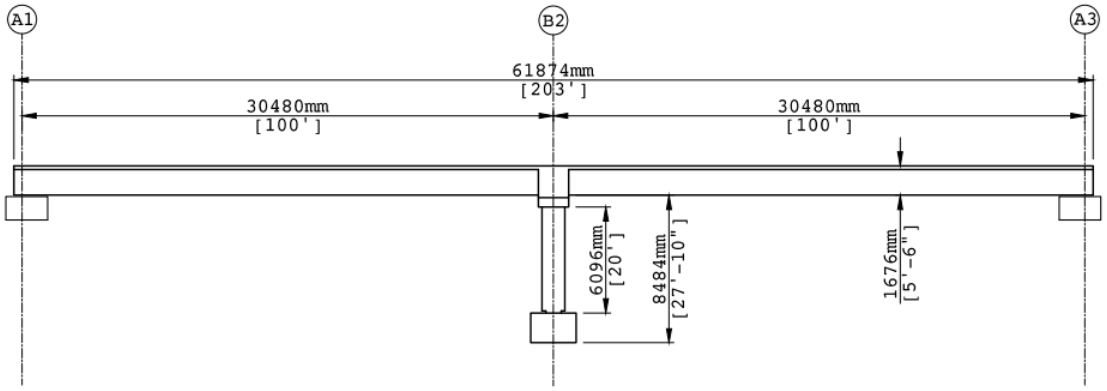

Figure 15: Elevation view of the suggested prototype bridge (Shoushtari et al., 2019)

All components of the prototype bridge were rescaled from the model to accommodate the larger structure. The prototype bridge has two equal spans of 100 ft (1200 in.) and is 31 ft (372 in.) wide. The bridge bent consists of two 4 ft (48 in.) diameter columns spaced 9 ft (108 in.) apart on-center and a 6 ft (72 in.) wide by 7.5 ft (90 in.) deep cap beam that spans the entire width of the bridge. The columns have a clear height of 20 ft (240 in) and are integral with the superstructure. The superstructure comprises four steel plate girders with a 9 in. deck overlay. The columns are designed to have a pinned connection at the base, and the abutments are seat-type abutments that restrain movement in the vertical direction. The weight of the prototype bridge consists of the overall weight of the columns, cap beam, and superstructure.

The prototype bridge was modeled in OpenSees using the same simplified wireframe model used for the scale model bridge. Figure 16 shows the plan and elevation views of the finite element model for the prototype bridge. The superstructure, cap beam, and columns are modeled using frame elements with concrete and steel materials. The material properties remained unchanged, and the elements were defined using larger cross-sections.

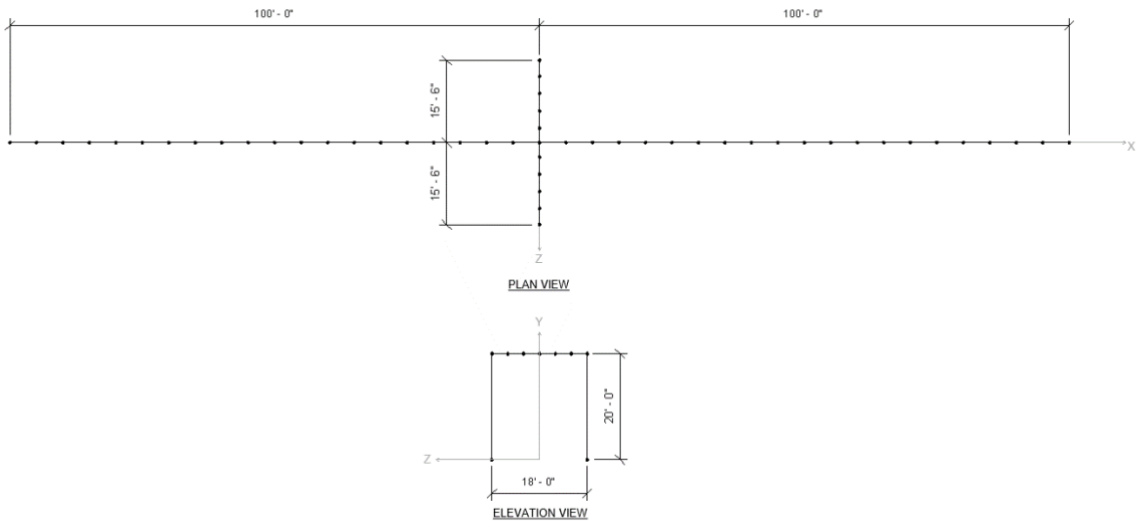

Figure 16: Plan and elevation views of the prototype finite element model.

The column section is a fiber section with a concrete core and circular layer of longitudinal reinforcement. The diameter of the column is 48 in. with reinforcement of 22 No. 11 bars with a 2 in. clear cover. Torsion is defined using the section's shear modulus and polar moment of inertia. Each column is defined as one displacement-based beam-column element. The top nodes are shared with the cap beam, and the bottom nodes are pinned. The mass of the column is divided in half and lumped at the top and bottom nodes.

The cap beam is a fiber section with a quadrilateral concrete patch and two layers of longitudinal reinforcement. The beam has a width of 6 ft and a height of 7.5 ft. The concrete patch covers the overall cross-section, and the reinforcement is defined as two layers of 50 No. 9 bars along the top and bottom of the section with a 2-inch. clear cover. The section aggregator defines the torsion in the beam by providing the shear modulus and polar moment of inertia. The cap beam consists of ten force-based beam-column elements, with the total mass of the beam evenly distributed at the nodes.

The deck and girders are defined separately along a single line of nodes. The superstructure was modeled again in SAP2000 to retrieve the correct section properties for the deck and girder. The deck overlay is 9 in. thick by 31 ft. wide with two layers of No. 3 rebar modeled as an elastic section. The deck spans the entire length of the bridge.

The four-steel girder design from the scale model is used for the prototype bridge. The girders are wide flange beams with a steel yield stress of 50 ksi and an elastic modulus of 29,000 ksi. The girders are spaced evenly across the width of the bridge, and the dimensions of the girders are scaled up from the model bridge. The dimensions for each girder are shown in Figure 17. The four girders are defined as a single element along the middle of the bridge. The cross-sectional area and moment of inertia about the y-axis and z-axis are determined from the SAP2000 model. The parallel axis theorem was used to calculate the overall moment of inertia about the y-axis and z-axis using the section properties for each girder.

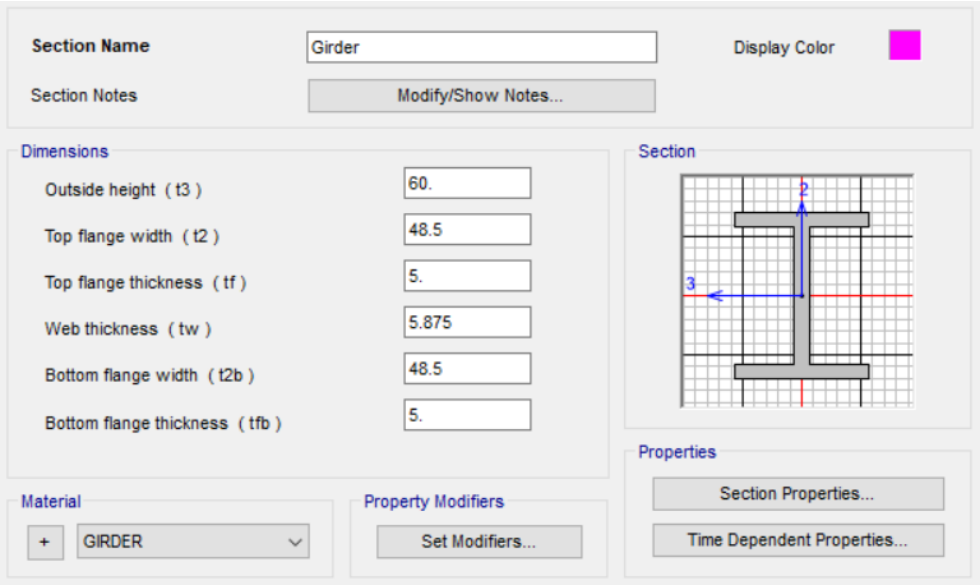

Figure 17: Dimensions used for girder design.

Table 6 shows the section properties used to define the deck and girders in OpenSees. The deck and girders are defined as separate elements along the same line of nodes. The end nodes of the superstructure are restrained in the vertical direction for the seat-type abutments.

Table 6: Section properties for deck overlay and steel girders.

Property	Deck	Girders
Area (in^2)	3393	3115
Iy (in^4)	946849	1753218
Iz (in^4)	38609136	60253960
J (in^4)	39555985	62007178

The total weight of the bridge is determined by all the structural components. The computed weight of each column and the cap beam are 37 kips and 210 kips, respectively. The weight of the superstructure is 2,794 kip which was determined by the SAP2000 model. For gravity loading, the weight is lumped at the nodes and applied in the vertical direction. The weight of each component is divided by gravity to determine the mass. The mass is lumped at the nodes and applied to the x-, y-, and z-coordinates. Gravity loading is applied to the system to set the structure's weight before dynamic loading.

The first three modes for the prototype model are in-plane rotation, longitudinal, and transverse, which agree with the model scale modal analysis. The first three periods associated with these mode shapes are listed in Table 7, which are comparable to those of a typical bridge.

Table 7: Periods for the first three mode shapes in model and prototype scales.

Mode	**Model Scale Period**	**Prototype Scale Period**
1	1.42 s	7.32 s
2	0.38 s	1.34 s
3	0.27 s	1.27 s

The prototype model in OpenSees was run with linear and nonlinear analyses to compare the responses under earthquake excitation. The linear analysis uses elastic beam-column elements and linear algorithm type to complete the analysis. The nonlinear analysis uses force-based beam-column elements and Newton algorithm type for analysis. Each run recorded the force-displacement results at the top of each column and time-displacement histories at the string potentiometer locations. Figure 18 shows the locations used to record the displacements along the bridge deck.

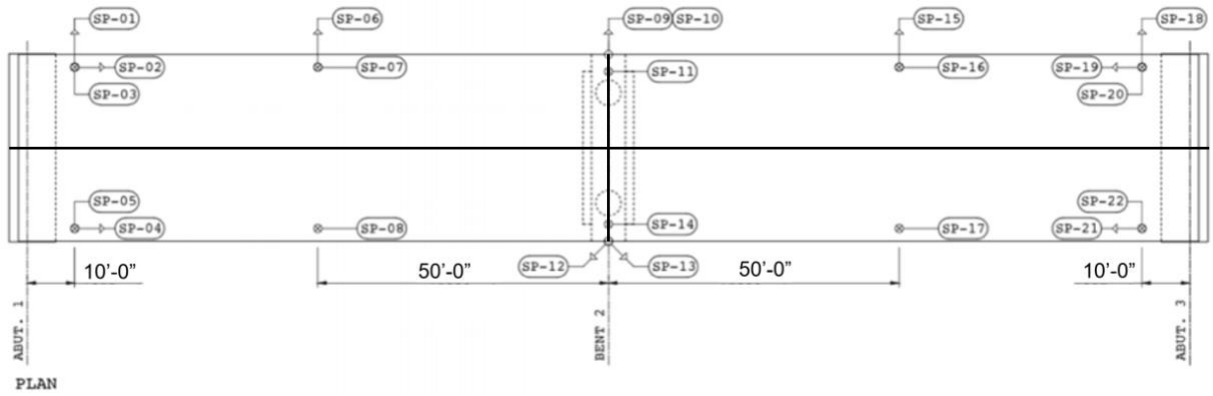

Figure 18: Visualization of the testing layout of string potentiometers along the bridge with wireframe overlay (from Shoushtari et al., 2019).

For the dynamic analysis, the model uses 6% damping. The OpenSees code uses the Newton algorithm to complete the nonlinear analysis. The analysis uses a tolerance of 0.005 and a maximum of 200 iterations at each time step. The displacement of each node and forces in the columns are recorded throughout the run and used to determine the bridge response.

The hysteresis loops are used to analyze the bridge response. The hysteresis loop is determined from the average of the recorded forces and recorded displacements at the top of each column. The recorded displacements are considered relative because the base of the columns is fixed. The forces

and displacements are averaged to estimate the response at the bridge's center. The following section will discuss the simulation results compared to the soil-bridge model.

Prototype Bridge Model on Soil Domain

The direct modeling approach was used for SSI modeling to develop a three-dimensional soil model. The soil model is 400 meters in the longitudinal direction (x-axis) and 200 meters in the transverse direction (z-axis). The model is 50 meters deep with two elevated surfaces to create approach ramps on either side of the bridge. Figure 19 shows a plan and elevation view of the soil domain.

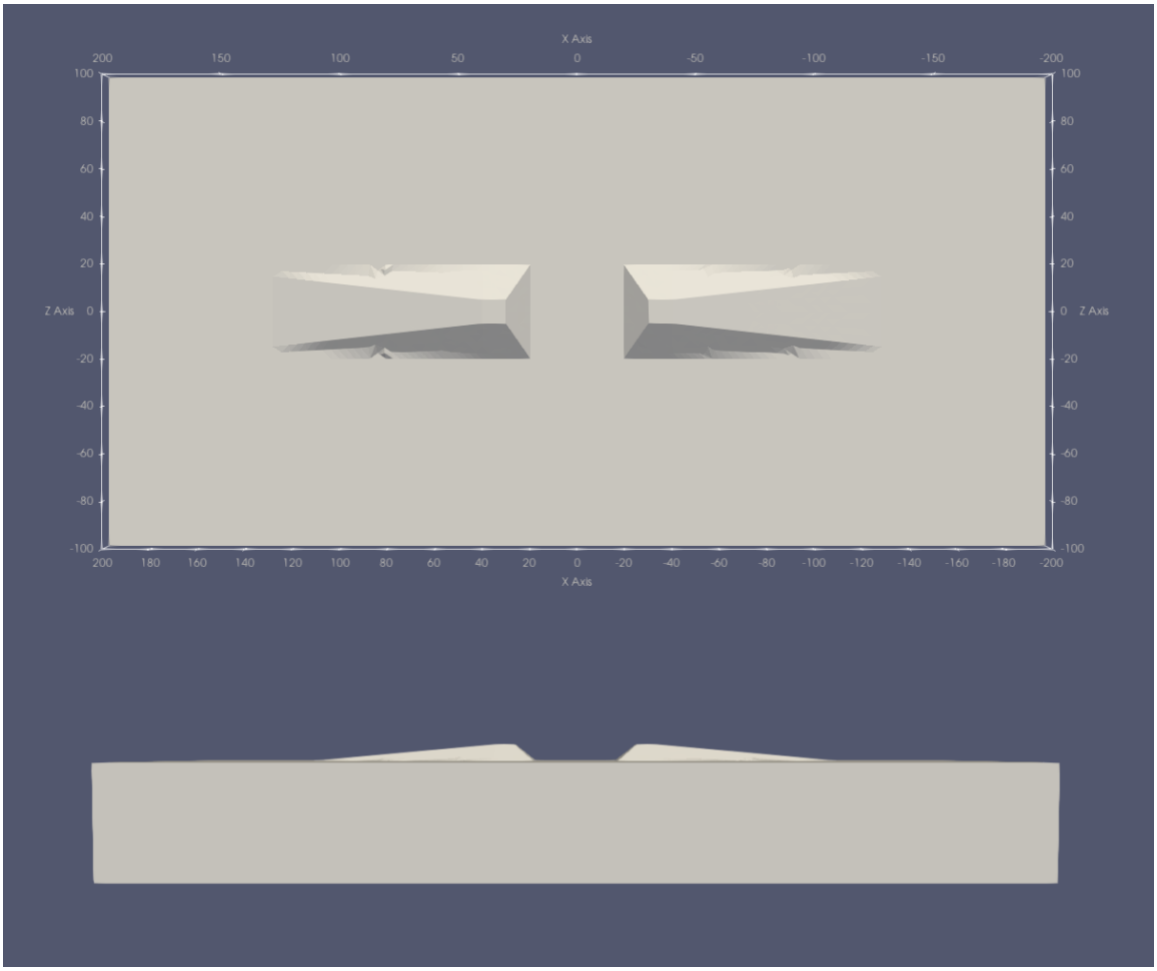

Figure 19: Plan and elevation views of the soil domain.

The direct modeling approach calls for modeling the excitation field and the truncation boundaries for absorbing outgoing waves. The domain reduction method (DRM) (Bielak et al., 2003) was used for modeling the excitation field, and a buffer zone with high damping layers was used for truncation. The DRM is not explicitly available in OpenSees. Therefore, we use the seismo-VLAB software (http://seismovlab.com) to generate the required nodal forces prescribed in the OpenSees model. The soil domain was tested separately to ensure the model responded correctly before combining the soil model with the prototype bridge to investigate the SSI effects.

The soil domain is modeled as a homogeneous medium with a shear wave velocity of 300 m/s, density of 2000 kg/m^{3,} and Poisson's ratio of 0.3. For modeling the seismic wavefield, inclined plane waves are considered, as shown in Figure 20. The soil displacement is shown as the wave travels through the domain, and the absorbing boundary is seen along the outer edges of the soil domain. To properly test the model performance in modeling wave propagation, the Ricker wavelet was used to define the temporal variation of arriving waves. The central frequency of the Ricker wavelet is 1Hz.

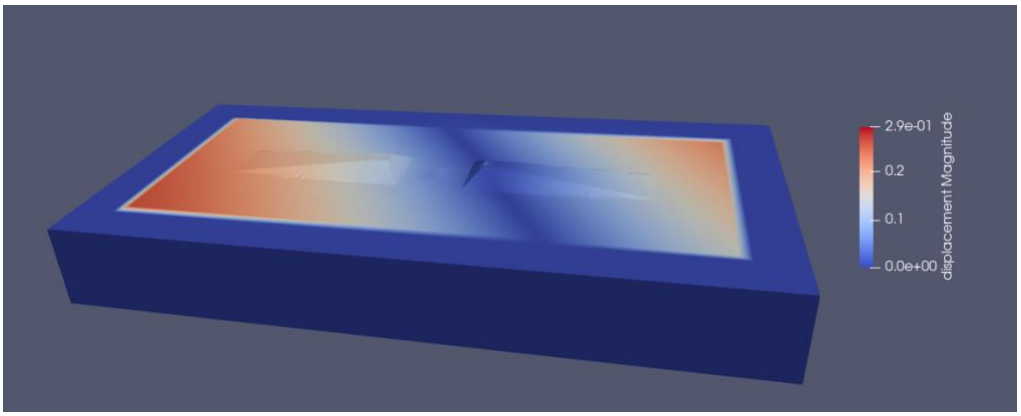

Figure 20: Wave propagation through the soil domain.

The bridge model is added to the existing finite element mesh for bridge-abutment-soil interaction analysis. The deck's end nodes are tied to the abutment for coupling the bridge and soil model. The

columns' bottom nodes are tied to the foundation to have the same displacement in the longitudinal, transverse, and vertical directions.

The foundation for the bridge is defined by the elements surrounding the nodes where the bridge columns connect to the soil. The foundation is defined as a slab with dimensions of 10 m x 10 m x 2.5 m defined by sixteen standard brick elements. The material is defined as "Elastic Isotropic" with a compressive strength of 41.4 MPa (6.0 ksi).

Due to the large size of the domain, the parallel version of OpenSees, i.e., OpenSees-SP, was used through the DesignSafe cyberinfrastructure at UT Austin. Based on preliminary analysis, it is noted that each simulation can take between one to two days to complete. The time-displacement histories and force-displacement responses are recorded similarly to the bridge-only case. After completing the SSI analysis under the simplified wavefield, the acceleration time series is recorded at the column foundation interface. Then, this base excitation is used to analyze the prototype bridge model. This allows the SSI effects to be studied more systematically.

Prototype Bridge Model Results with and without SSI Effects

Both developed bridge models were analyzed using input motion from an earthquake event. Figure 21 shows the input motion used for analysis. The acceleration was recorded from the soil domain at the foundation level (without bridge) and converted into units of inches per second squared (in/s^2) to use as input for the bridge-only case. The earthquake motion runs for 20 seconds, with the highest acceleration between four and ten seconds. The earthquake motion was used to compare the bridge-only case and bridge+soil case. The comparison of linear and nonlinear force-displacement responses between the bridge-only and bridge+soil cases are shown in Figures 22 and 23, respectively. The bridge+soil case shows similar results in the transverse direction to the

bridge-only case. The longitudinal responses show that the bridge+soil model does not reach the same maximum force and displacement as the bridge-only case.

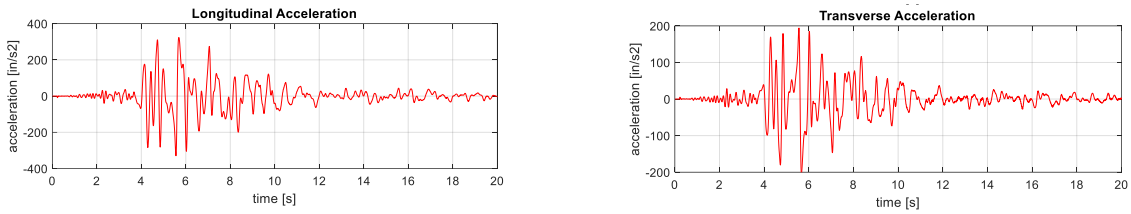

Figure 21: Input earthquake motion.

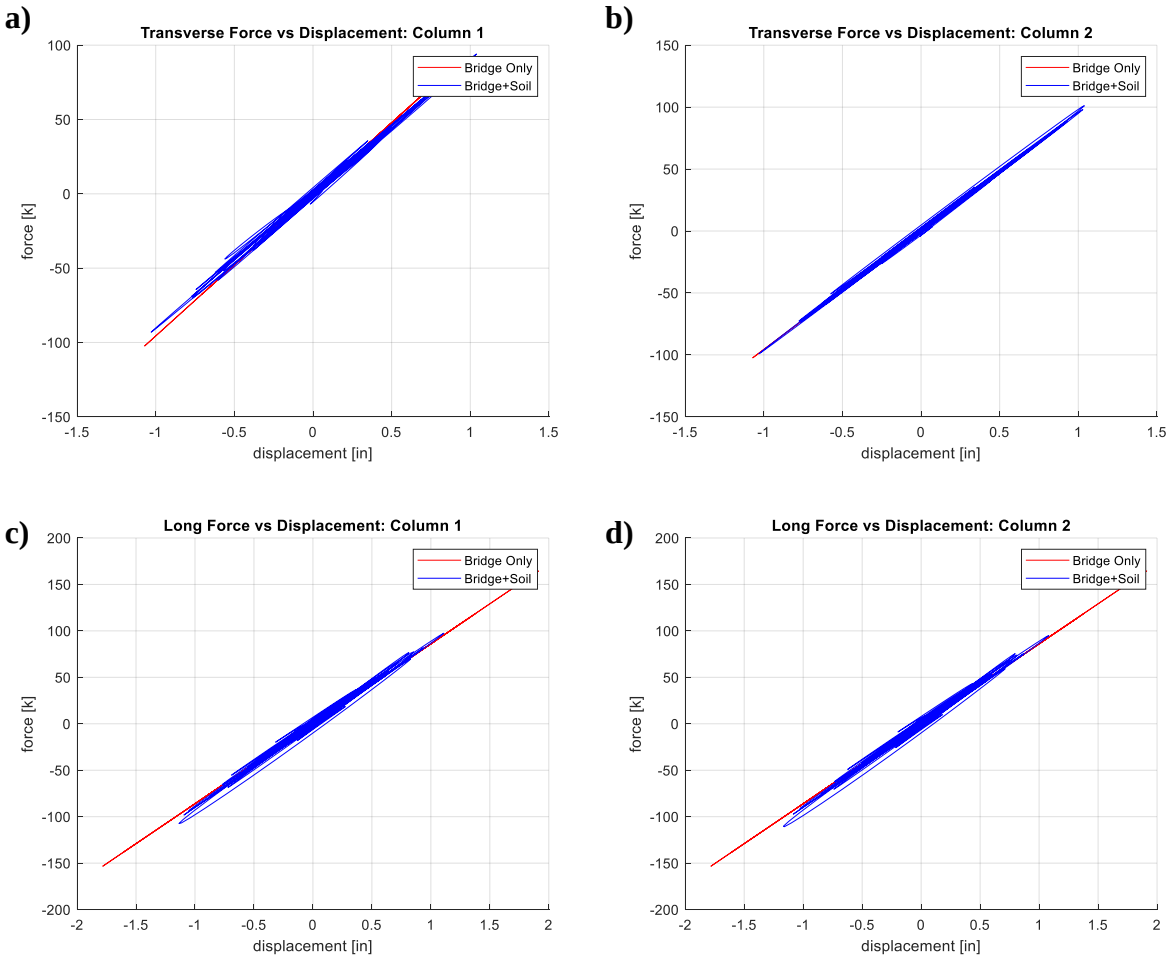

Figure 22: Linear force-displacement comparisons for a) column 1 transverse motion, b) column 2 transverse motion, c) column 1 longitudinal motion, and d) column 2 longitudinal motion.

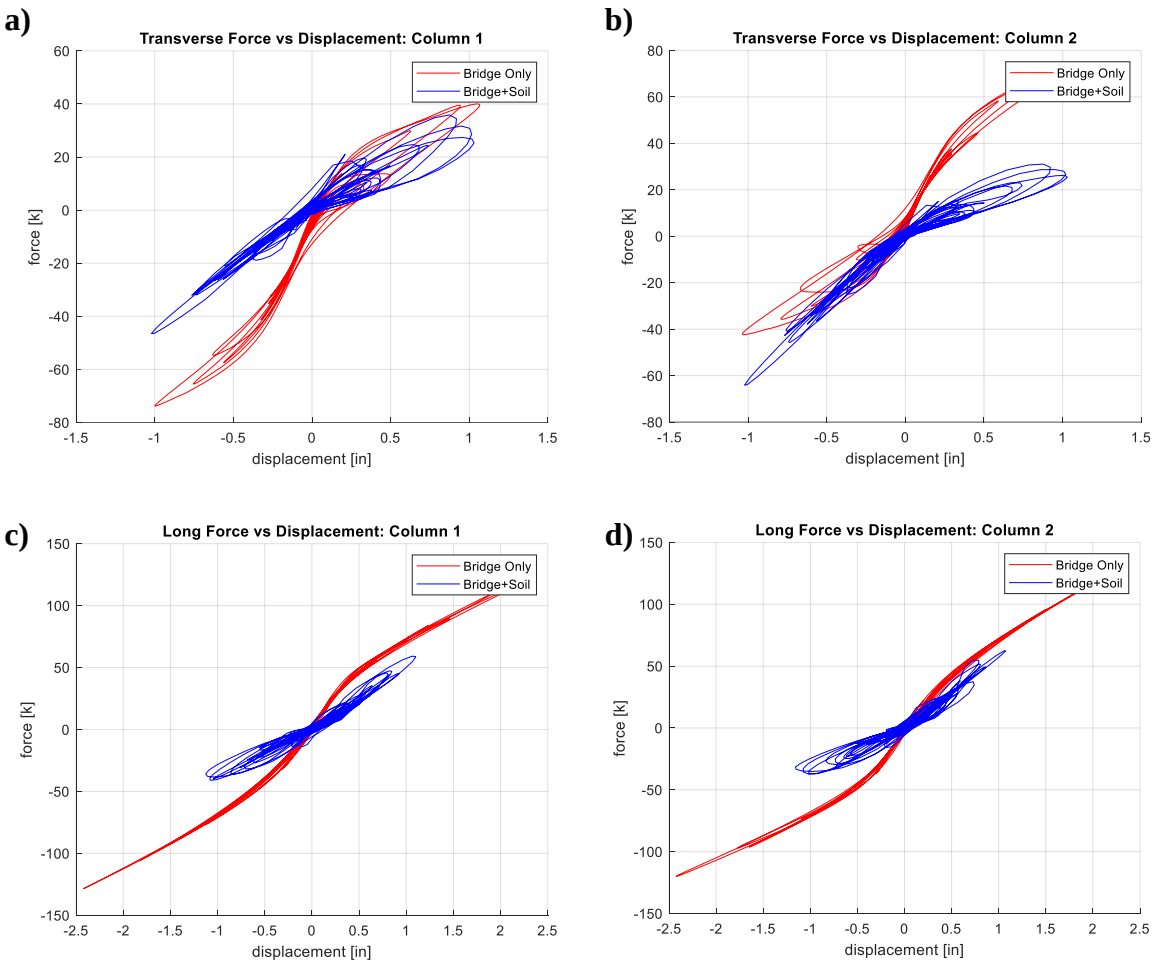

Figure 23: Nonlinear force-displacement comparisons for a) column 1 transverse motion, b) column 2 transverse motion, c) column 1 longitudinal motion, and d) column 2 longitudinal motion.

The displacements of the systems were also recorded and compared at specified locations along the bridge. Figures 24 and 25 compare the displacements for both cases for linear and nonlinear responses. Due to the soil flexibility and radiation damping, the bridge+soil response is not as significant as the bridge-only case.

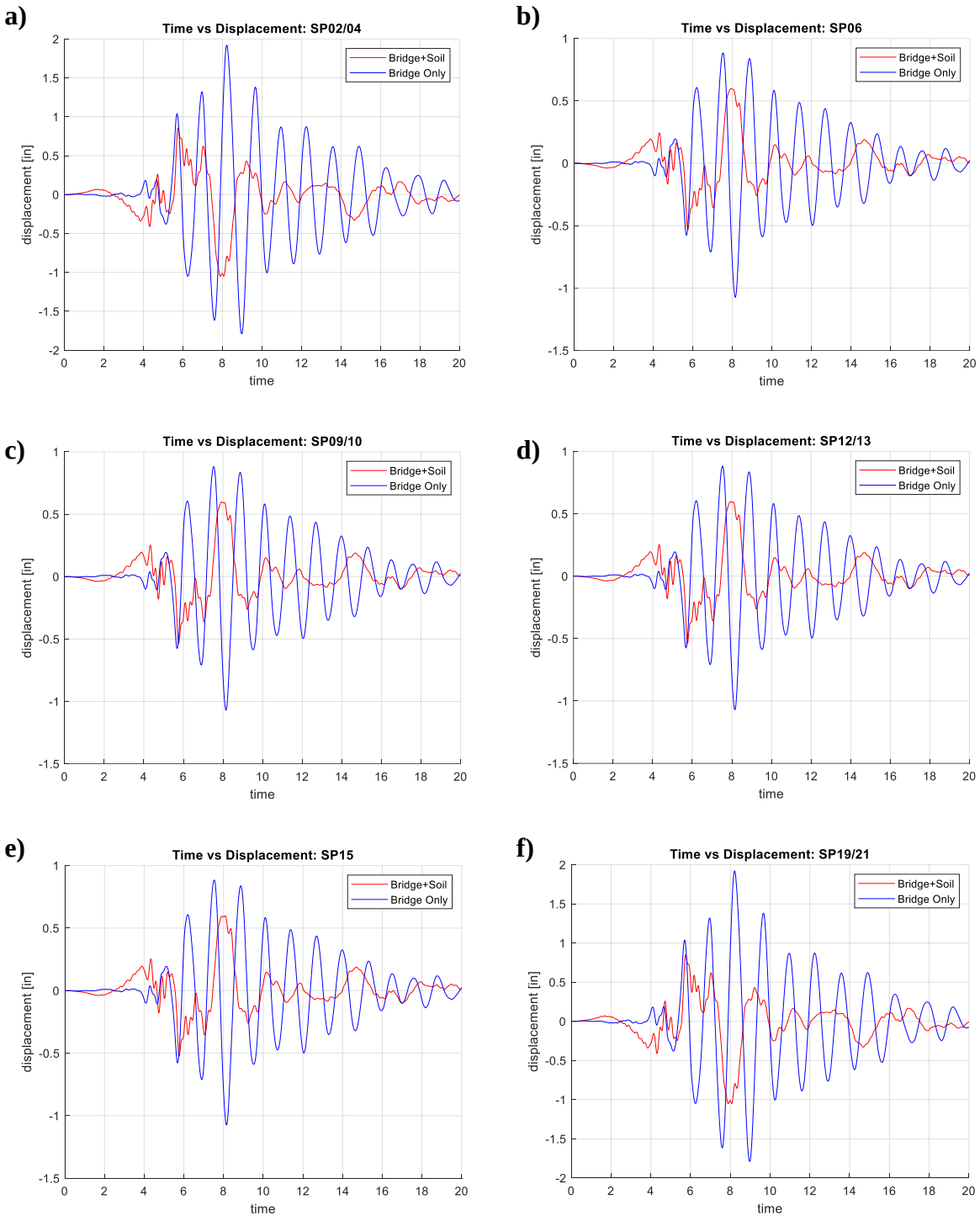

Figure 24: Linear time-displacement histories for both cases at a) SP02/04, b) SP06, c) SP09/10, d) SP12/13, e) SP15, and f) SP19/21.

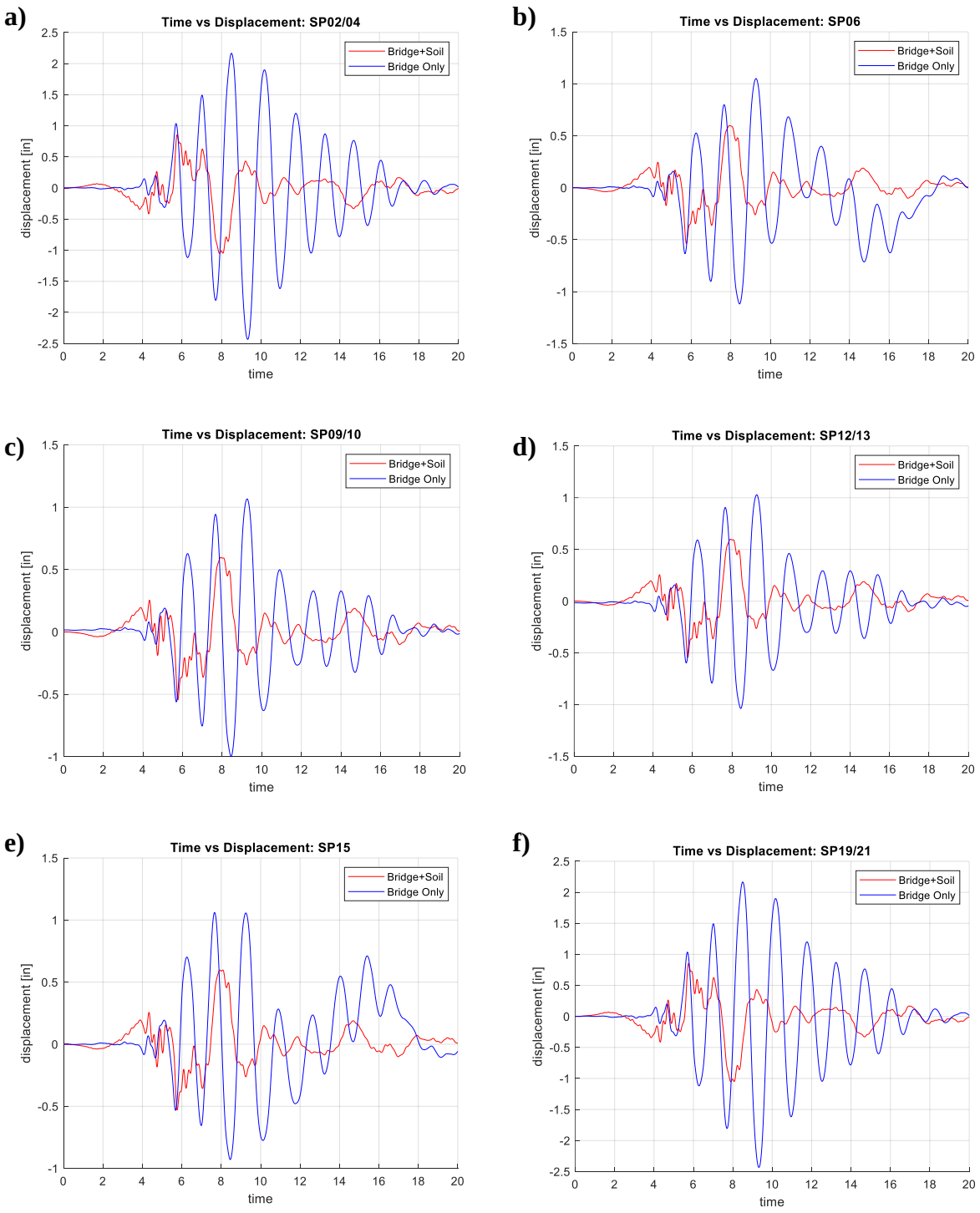

Figure 25: Nonlinear time-displacement histories for both cases at a) SP02/04, b) SP06, c) SP09/10, d) SP12/13, e) SP15, and f) SP19/21.

SSI Effects on ABC Connections

The model bridge tested at UNR incorporated six different ABC connections into the design. The overall bridge design was based on the AASHTO LRFD Bridge Design Specifications. The ABC connection design was based on emerging methods published in multiple research articles before the project. For the premises of this project, the ABC connections were simplified within the OpenSees model. The simplified model used the same materials and material properties as the tested bridge. The analytical studies showed that the simplified bridge model successfully captured the experimental results of the previously tested model bridge.

The two-column bent was designed using two ABC connection types: a two-way hinge connection and grouted duct connection. The two-column bent used in the bridge model was designed with precast footing and columns. The footing was precast with two pockets made from a corrugated metal pipe for the columns to be placed. The columns were placed into the footing pockets and filled with high-strength non-shrink grout to form the two-way hinge connection. The columns were embedded 19 inches into the footing to achieve the minimum embedment length for the column longitudinal bars. A gap of 1.5 inches was provided between the columns and footing to allow for column rotation and to create a pinned connection. For simplification of the connection, the base of the columns in the OpenSees model was fixed for the bridge-only case and tied to the soil nodes for the bridge+soil case. Shoushtari et al. (2019) provided a schematic in Figure 26 that illustrates the connection between the column-footing interface and column-cap beam interface. The cap beam consisted of a precast drop for the bottom section and was cast in place for the top section. The precast drop provided metal ducts at the column locations to allow the longitudinal column reinforcement to pass through the section. The precast beam was placed on top of the columns, and the ducts were filled with high-strength grout to create the grouted duct connection.

The longitudinal column bars were embedded deep enough for bar development. The top section of the cap beam was cast in place to form the connection to the bridge deck elements.

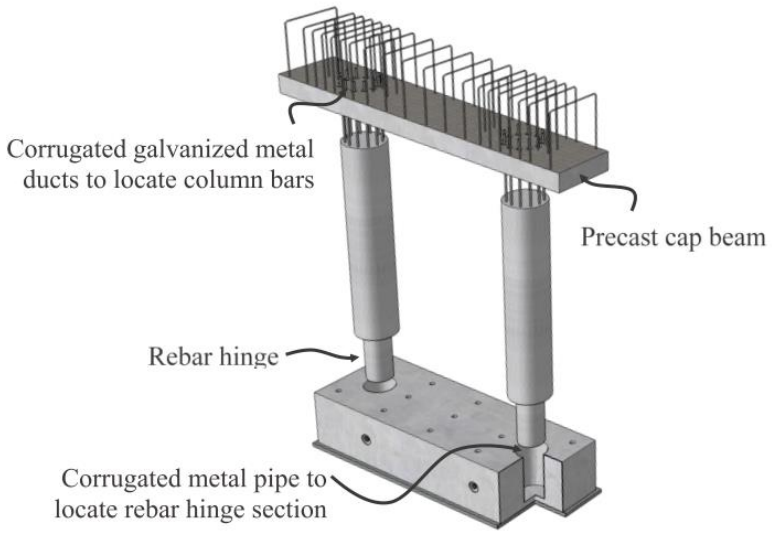

Figure 26: Schematic of ABC column connections (Shoushtari et al., 2019)

For the simplified OpenSees model, the nodes at the top of the column elements share nodes with the cap beam to form the connection. All elements were modeled as "ForceBeamColumn" elements, allowing for the spread of plasticity along the element. The columns were designed as a fiber section with a 4-foot diameter and a longitudinal steel ratio of 1.86% to satisfy AASHTO requirements. The minimum embedment length for bar development is accounted for with the depth of the cap beam. The cap beam is modeled as a single fiber section 6 feet wide and 7.5 feet deep for simplification. The nonlinear results of the bridge cases show that the maximum displacement at the top of the column is 2.5 inches. This displacement corresponds to a 1.5% drift ratio, which is relatively small. Due to the relatively small drift ratio, the design of the column footing and column-cap beam interfaces can be determined as adequate for the loading.

The OpenSees model records the force in each column element for bridge only and bridge+soil cases. The recorded forces determine the percentage of change between the cases at the specified

interfaces. Table 8 shows the maximum shear forces recorded at the two interfaces for linear and nonlinear analysis. The differences between the forces are shown with a percentage of change.

Table 8: Recorded shear forces from the OpenSees model at column interfaces.

	Location	Analysis	Direction	Bridge Only (k)	Bridge+Soil (k)	Change (%)
Column 1	Column-Cap Beam Interface	Linear	Longitudinal	164.47	107.38	**34.71%**
			Transverse	93.72	94.02	**0.32%**
		Nonlinear	Longitudinal	128.53	59.22	**53.93%**
			Transverse	70.56	68.29	**3.22%**
	Column-Footing Interface	Linear	Longitudinal	164.47	107.38	**34.71%**
			Transverse	93.72	94.02	**0.32%**
		Nonlinear	Longitudinal	128.53	59.22	**53.93%**
			Transverse	70.56	68.29	**3.22%**
Column 2	Column-Cap Beam Interface	Linear	Longitudinal	164.47	110.79	**32.64%**
			Transverse	111.83	101.13	**9.57%**
		Nonlinear	Longitudinal	124.06	62.37	**49.73%**
			Transverse	72.94	64.08	**12.15%**
	Column-Footing Interface	Linear	Longitudinal	164.47	110.79	**32.64%**
			Transverse	111.83	101.13	**9.57%**
		Nonlinear	Longitudinal	124.06	62.37	**49.73%**
			Transverse	72.94	64.08	**12.15%**

The longitudinal direction shows more significant differences between the bridge-only and bridge+soil cases. The percent of change is approximately 33% and 52% for linear and nonlinear analyses, respectively. The shear force is reduced in the bridge+soil case due to the presence of the soil. For the bridge-only case, the abutments are modeled as "rollers" and are free to move in the longitudinal and transverse directions where the abutments are tied to the soil in the bridge+soil model. The reduction of a shear force applied at the interfaces shows that the connections are designed for higher forces than what will be seen in the presence of soil for the configuration studied in this project. For the transverse direction, the linear analysis shows a more minor change in force between the two cases than the nonlinear analysis. The minor change in force is because the transverse movement of the bridge is not as affected due to the seismic waves traversing in the

longitudinal direction. The transverse forces differ between the columns due to the in-plane rotation of the bridge deck.

Overall, the demands for the connections are significantly decreased when considering the soil profile attached to the base of the bridge. The slight deformation of the bridge proves that the bridge materials and connections were designed adequately for a realistic seismic event studied in this project. The OpenSees model captured the bridge response with sufficient accuracy at the scale model level, allowing us to conclude that the prototype model can estimate the response of a full-scale ABC bridge with an analytical model.

References

Bielak, J., Loukakis, K., Hisada, Y., & Yoshimura, C. (2003). Domain reduction method for three-dimensional earthquake modeling in localized regions, Part I: Theory. *Bulletin of the seismological Society of America*, *93*(2), 817-824.

Kwon, O. S., & Elnashai, A. S. (2008). Seismic analysis of Meloland road overcrossing using multiplatform simulation software, including SSI. *Journal of Structural Engineering*, *134*(4), 651-660.

McKenna, F., Scott, M. H., & Fenves, G. L. (2010). Nonlinear finite-element analysis software architecture using object composition. *Journal of Computing in Civil Engineering*, *24*(1), 95-107.

Mylonakis, G., Nikolaou, A., & Gazetas, G. (1997). Soil–pile–bridge seismic interaction: kinematic and inertial effects. Part I: soft soil. *Earthquake engineering & structural dynamics*, *26*(3), 337-359.

Rahmani, A., Taiebat, M., & Finn, W. L. (2014). Nonlinear dynamic analysis of Meloland Road Overpass using a three-dimensional continuum modeling approach. *Soil Dynamics and Earthquake Engineering*, *57*, 121-132.

Shoushtari, E., Saiidi, M. S., Itani, A. M., & Moustafa, M. A. (2019). *Shake Table Studies of a Bridge System with ABC Connections* (No. ABC-UTC-2013-C2-UNR04-Final). Accelerated Bridge Construction University Transportation Center (ABC-UTC).